Title

MASS TRANSFER IN TURBULENT FLOW BETWEEN ROTATING CYLINDERS WITH SMALL SEPARATION GAPS

Permalink

https://escholarship.org/uc/item/6817n8z5

Author

Mohr Jr., Charles M.

Publication Date

1976-05-01

Submitted to Electrochimica Acta

LBL-5136 c.1
Preprint

MASS TRANSFER IN TURBULENT FLOW BETWEEN ROTATING CYLINDERS WITH SMALL SEPARATION GAPS

Charles M. Mohr, Jr. and John Newman

May 1976

Prepared for the U. S. Energy Research and
Development Administration under Contract W-7405-ENG-48

DISCLAIMER

LBL-5136

Mass Transfer in Turbulent Flow between Rotating Cylinders with Small Separation Gaps

Charles M. Mohr, Jr., and John Newman

Materials and Molecular Research Division, Lawrence Berkeley Laboratory,
and Department of Chemical Engineering, University of California,
Berkeley, California 94720

May, 1976

Abstract

The results of an experimental study of mass transfer in turbulent cylindrical Couette flow are presented and compared to the predictions of a model based upon the empirical "universal velocity profile" derived for turbulent pipe flow. The gap distance between the nickel electrodes was varied from nine percent to less than two percent of the inner cylinder radius, and the experiments were performed using the ferricyanide-ferrocyanide redox reaction in KOH and $NaOH/Na_2SO_4$ supported electrolytes. The mass-transfer rates were found to lie below those predicted by correlations of data from wider gap experiments and displayed fundamental differences from the predictions of the proposed model. For the limited range of parameters, Re (Reynolds number) and κ (gap ratio), studied, the data (for a Schmidt number of 1661) are fit to within ±4% by the equation

$$St = (0.001177 - 0.000983\kappa)Re_i^{-0.2}$$

where St is the dimensionless Stanton number. The results suggest that the "universal velocity profile" is not applicable to this flow and that further modeling advances for this system must be based upon an improved knowledge of the nature of rotating turbulent flows.

Key words: limiting current

Introduction

The electrode system employing concentric rotating cylinders offers considerable promise for electrochemical investigations. While its advantages are many: uniform potential, current, and concentration distributions at the working electrode surface and the capability of building a system with relatively high surface area per unit volume of solution (for a non-porous electrode), it suffers from a serious handicap that has prevented its widespread adoption as an experimental tool. That is, the mass-transfer behavior of this sytem is not described sufficiently well to allow accurate determination of the interfacial concentration from current and bulk concentration measurements. The suppression of natural convection in this system dictates the use of high rotation speeds (usually for the inner cylinder while the outer one remains stationary) so that turbulent flow conditions prevail. While the behavior of rotating turbulent flows has received some attention, the empirical treatment of this situation does not appear to be sufficiently advanced to allow its immediate usage to predict friction-factor and mass-transfer behavior in such flows.

Gabe(1) has recently reviewed the several studies that have been directed toward resolving the experimental correlation for mass transfer in this system. The pioneering work in this field was performed by Eisenberg,(2,3) and his correlation for the mass-transfer dependence upon the system and solution parameters has been substantiated by subsequent investigations.(4-7) For all systems that appear to have been studied to date, the gap between the inner and outer cylinders has comprised a significant portion of the outer cylinder radius:

$$0 < \kappa \leq 0.85 \tag{1}$$

where $\kappa = R_i/R_o$ and R_i and R_o are the inner and outer cylinder radii respectively. These studies concluded that the mass transfer and friction factor(8) could be correlated best with a Reynolds number based on the inner cylinder radius

$$Re_i = \frac{R_i^2 \Omega}{\nu} \tag{2}$$

where Ω is the rotation speed of the inner cylinder and ν is the kinematic viscosity of the solution. This result is not anticipated by traditional views of shear-induced turbulence, which would lead one to expect that the proper Reynolds number for a best fit would be based upon the gap dimension,

$$Re = \frac{R_i(R_o - R_i)\Omega}{\nu} , \tag{3}$$

rather than the form given in equation 2. The classic stability study of Taylor(9) has demonstrated that the proper dimensionless group for correlating the point of instability of the simple cylindrical Couette flow is

$$Ta = \frac{R_i(R_o - R_i)\Omega}{\nu}\sqrt{\frac{R_o - R_i}{R_i}} \qquad (4)$$

as given by Schlicting;(10) Ta is the "Taylor" number. The similarity between this group and the gap-distance based Reynolds number, equation 3, is apparent.

This study has been performed to investigate the small-gap mass-transfer behavior for such rotating cylinder systems and to test whether or not current empirical models for the structure of shear-induced turbulence are appropriate for such small gaps. While Gabe and Robinson(11) have suggested that for small gaps the gap size must eventually become significant, the form that this influence may take has not yet been elucidated by previously published studies.

Experimental Measurements of Mass Transfer in Turbulent Cylindrical Couette Flow

Electrode Reactions

The oxidation-reduction reactions involving ferricyanide and ferrocyanide ions were chosen for this investigation. Eisenberg(3) has discussed these reactions and has shown that their use with nickel electrodes provides excellent limiting-current behavior when hydrogen evolution is suppressed through the use of an alkaline supporting electrolyte. Accordingly, NaOH and KOH were used in this study as supporting electrolytes.

Equipment

Eisenberg's original equipment was modified to meet the needs of this study. A schematic drawing of the cell is given in figure 1. The drive mechanism and peripheral electronic equipment are described elsewhere.(12) The nickel electrode sizes were chosen to emphasize the influence of small gaps upon the transfer rate. The outer electrode was 136.65 mm in internal diameter. The four inner cylinders ranged from 124.5 to 134.4 mm in diameter, resulting in gap ratios, R_i/R_o, of from 0.916 to 0.983. Due to the decreased gap sizes, viscous dissipation was more pronounced in this study than in Eisenberg's, so a more efficient method of cooling the solution was required. While Eisenberg reported that adequate temperature control could be achieved by blowing hot or cold air on the cell, it was found necessary here to install a water jacket on the outer electrode in order to control the temperature to within the 0.2°C claimed by Eisenberg. Another modification found useful was the installation of a circulating pump and thermometer chamber to monitor the cell temperature, since the thin gaps did not allow direct insertion of a thermometer. The pump was a Teel model 1P579 general purpose positive displacement pump which circulated solution drawn from the bottom of the cell past the thermometer and returned it to the top of the cell. Pumping rates were high enough to affect noticably the values of the limiting currents, so the pump was turned off before measurements were made.

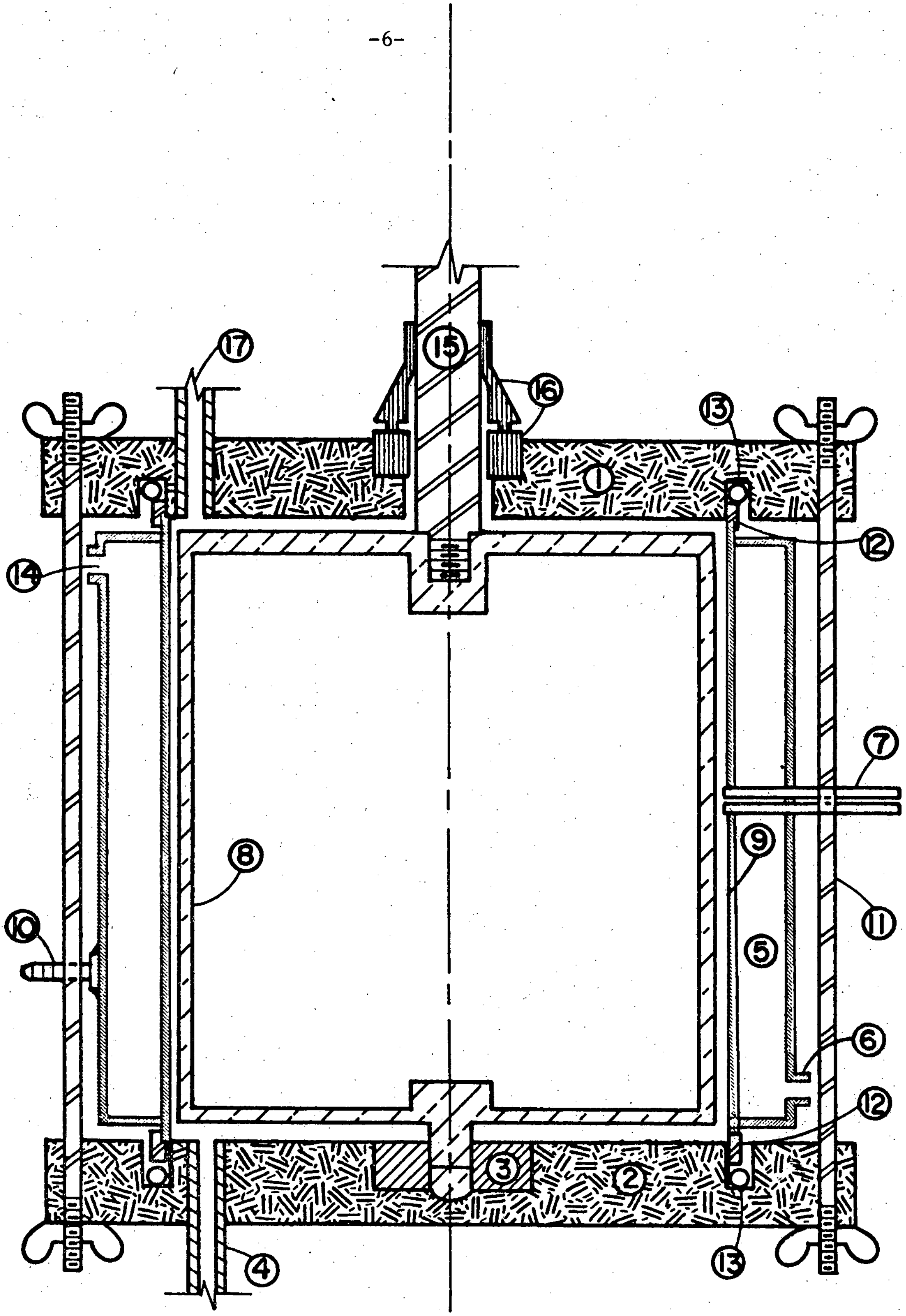

Figure 1. Schematic of equipment.

XBL756-3100

Cell and Electrode Nomenclature for Figure 1

1 Plexiglass top of cell.

2 Plexiglass bottom of cell.

3 Teflon bearing.

4 Outlet from cell (to pump and thermometer container).

5 Brass water jacket.

6 Cooling water inlet to 5 .

7 Glass capillary to reference electrode.

8 Nickel inner rotating cylinder.

9 Nickel outer cylinder welded to 5 .

10 Threaded stud for contact to counterelectrode lead, soldered to water jacket.

11 3.175 mm threaded stainless steel rod, securing top and bottom of cell to outer electrode, fastened with wing nuts.

12 Stainless steel edge on nickel outer electrode.

13 Buna "O" ring seals.

14 Cooling water jacket outlet.

15 Stainless steel shaft, threaded to fit inner electrode.

16 Spring loaded rotating seal.

17 Entrance for solution from thermometer chamber.

The exact centering of the inner electrode can present a problem in this geometry. Any offset from the concentric alignment of the electrodes could be quite significant in this investigation since very small gaps (1.27 to 6.35 mm) were employed. Caliper and micrometer measurements indicated that the inner cylinders were of uniform radius (to within less than 25.4 μm) and that the internal diameter of the outer cylinder was 136.65 ± 0.025 mm. The cell could be centered relative to the rotating shaft to within approximately 76.2 μm and "run-out" in the rotating shaft with the cell and electrode in place was less than 25.4 μm as measured by a dial indicator with its point inserted in the access port for the capillary lead to the counterelectrode. This results in a possible deviation of less than 127 μm, a maximum percent deviation of less than ten percent for the smallest gap tested.

Surface roughness is another potential difficulty. A Gould "Surfanalyzer" was used to determine a typical roughness profile for the electrodes. A scan of a typical segment of inner cylinder radius is shown on figure 2. Surface deviation appears to be approximately 0.5 μm, which should cause no appreciable effect upon the mass transfer according to the results of Kappesser, Cornet, and Greif,(5) who determined that for

$$R_i/\varepsilon > 10^5 ,$$

where ε is the magnitude of the surface irregularities, the surface behaved in a "smooth" manner and the results for mass transfer followed the prediction of Eisenberg et al.

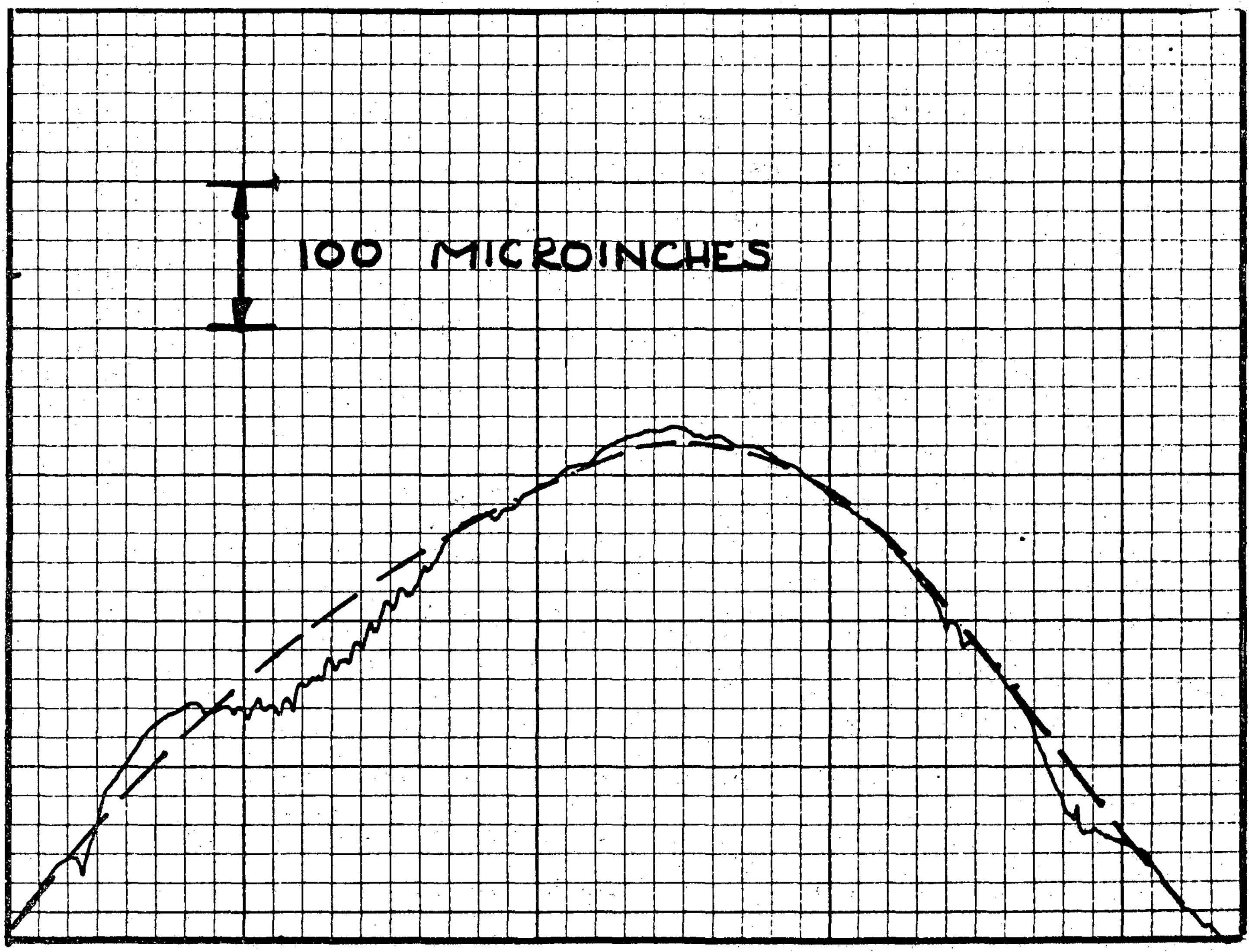

XBL 754-1109

Figure 2. Typical surface profile of inner cylindrical electrode.

Procedure

Prior to each run a fresh solution was prepared, and the electrodes were polished and washed. The electrode preparation scheme used by Eisenberg(3) was followed, except that cathodic treatment of the electrodes in a five percent NaOH solution was not performed. Eisenberg indicates that this is required for accurate determination of the kinetic parameters for the reaction but does not affect the limiting-current measurements.

The solution was introduced into the cell through the reference electrode reservoir; the air being forced out through a bleed line at the top of the thermometer chamber. The circulation pump was started, and the cylinder rotated at approximately 1000 RPM to allow viscous dissipation to heat the solution to 25°C. Manual control of the cooling water (industrial cold tap water) was found adequate to maintain the temperature of the solution at 25.0 ± 0.2°C. When temperature control was achieved at the rotation speed of interest, the circulating pump was turned off. A short delay allowed bubbles introduced by the pumping to leave the solution in the gap, after which a current scan using the ramp galvanostat was made. Scan rates were between 2 and 5 amperes/minute. A set of the resulting polarograms is shown on figure 3. The scan was halted when the limiting current plateau was reached since hydrogen evolution tended to alter the concentrations of the solution. Some change in the ferricyanide concentration seems unavoidable due to oxygen evolution at the anode. Eisenberg's measurements of the limiting currents for

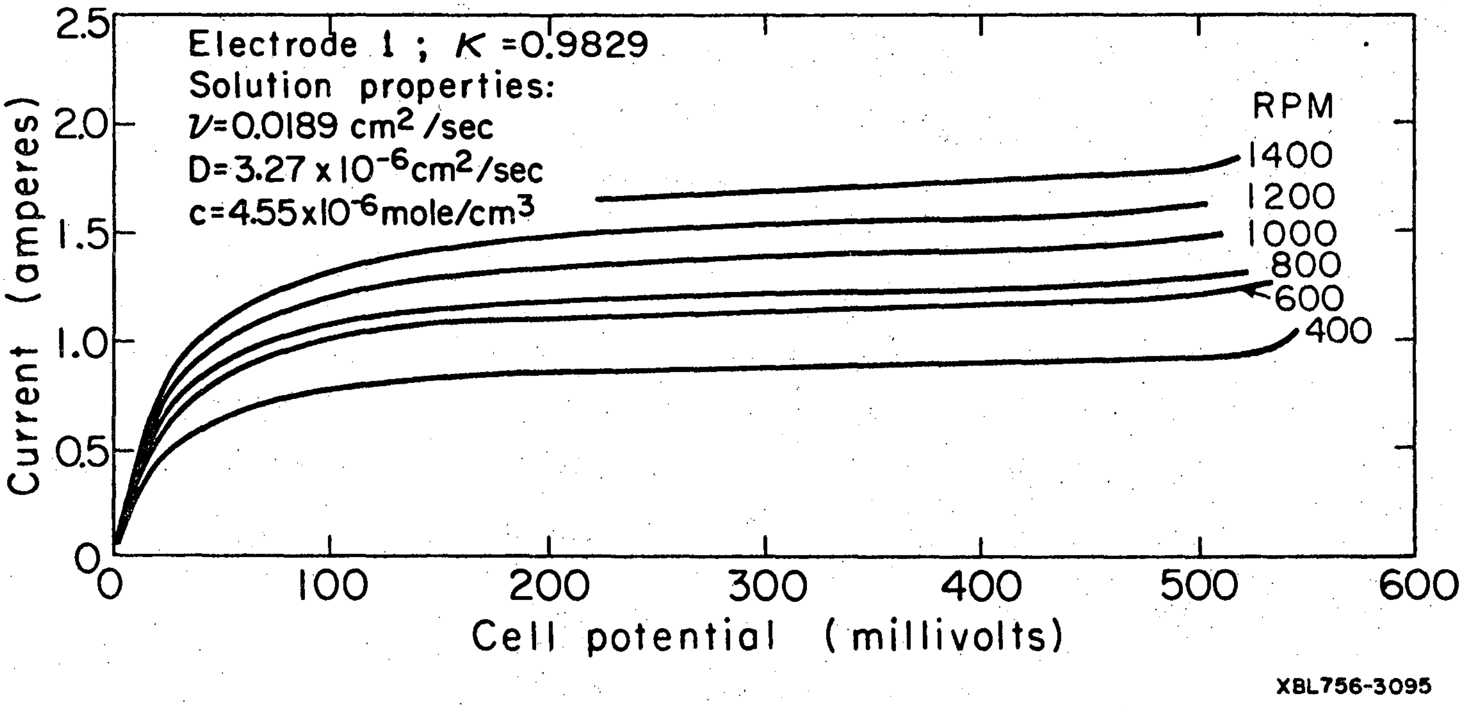

Figure 3. Typical polarograms for turbulent mass transfer between rotating cylinders.

the oxidation of ferrocyanide indicated a very poor plateau, demonstrating the presence of oxygen evolution. Thus the solutions were gradually depleted of ferricyanide, which made necessary periodic determination of the ferricyanide concentration. The iodometric titration for ferricyanide described by Kolthoff(13) was employed. Preparation of the solutions required for the titrations is discussed by Swift.(14)

Physical Properties of the Electrolyte Solutions

Two different solutions were used so that the Schmidt number of the solutions could be varied. The less viscous solution, which was used for most of the experiments, consisted of

0.0047 mole/ℓ $K_3Fe(CN)_6$
0.0050 mole/ℓ $K_4Fe(CN)_6$
and 0.850 mole/ℓ KOH .

The kinematic viscosity of these solutions was determined using an Ubbelohde capillary viscometer and was found to be $0.00952\ cm^2/sec$. The diffusion coefficient was determined using a nickel rotating disk electrode and was found to be $5.73\times10^{-6}\ cm^2/sec$. Both these values were measured at a temperature of 25.0°C.

The second solution consisted of

0.0047 mole/ℓ $K_3Fe(CN)_6$
0.0050 mole/ℓ $K_4Fe(CN)_6$
1.500 mole/ℓ Na_2SO_4
and 0.500 mole/ℓ NaOH .

The kinematic viscosity and diffusivity were found to be 0.0189 cm^2/sec and 3.27×10^{-6} cm^2/sec, respectively, at 25°C. The Schmidt number of this solution was 5780, compared to a value of 1661 for the first solution. This second solution appeared to have a rather short useful lifetime. While it remained clear for approximately twenty-four hours following its use in the cylinder device, small crystals of precipitate were noticed after this time and could not be redissolved. More concentrated Na_2SO_4 solutions were prepared (2.0 M), but they exhibited this tendancy to form a precipitate after an even shorter time -- less than one half hour. These solutions were abandoned due to the undesirable prospect of precipitation in the apparatus during the runs. While this use of Na_2SO_4 to vary the Schmidt number of ferricyanide, ferrocyanide solutions seems to be quite promising, this tendancy toward precipitation is clearly undesirable, and for experiments of lengthy duration, perhaps less concentrated solutions (~1 M) might prove more practical. The presence of the large amount of Na_2SO_4 had no apparent effect upon either the limiting current curves or the ferricyanide titration results.

Experimental Results

The data gathered for the runs performed are given in tables 1 and 2. Dimensionless mass-transfer rates are presented as Stanton numbers

$$St = \frac{\bar{i}}{nFR_1\Omega c}$$

where $\bar{i}$ is the average current density, n the number of electrons

Table 1: Experimental results for mass transfer between rotating cylinders; Sc = 1661.

Gap Ratio	rpm	$10^6 c$ mol/cm^3	$10^{-5} Re_i$	$10^5 St$
.9828	400	3.89	1.984	2.280
.9828	600	3.89	2.977	1.937
.9828	800	3.89	3.969	1.741
.9828	1000	3.89	4.961	1.512
.9828	1200	3.89	5.953	1.463
.9828	1400	3.89	6.946	1.419
.9607	1400	3.82	6.637	1.593
.9607	1600	3.72	7.585	1.581
.9607	400	3.62	1.896	2.143
.9607	600	3.62	2.844	1.920
.9607	800	3.62	3.792	1.809
.9607	1200	3.45	5.688	1.659
.9607	1400	3.35	6.637	1.681
.9607	1000	3.55	4.740	1.676
.9394	250	4.13	1.133	2.783
.9394	400	4.13	1.813	2.287
.9394	600	4.09	2.719	2.016
.9394	800	4.04	3.625	1.918
.9394	1200	3.90	5.438	1.802
.9394	1000	3.99	4.532	1.834
.9161	700	4.13	3.017	2.254
.9161	600	4.13	2.586	2.257
.9161	500	4.13	2.155	2.357
.9161	400	4.13	1.724	2.472
.9161	265	4.13	1.142	2.888
.9161	175	4.13	0.754	3.676
.9161	1000	4.13	4.311	2.093
.9161	1200	4.21	5.173	2.093
.9161	1000	4.21	4.311	2.099
.9161	800	4.21	3.448	2.118
.9161	400	4.21	1.724	2.524
.9161	250	4.15	1.078	2.830

Table 2: Experimental results for mass transfer between rotating cylinders; Sc = 5780.

Gap Ratio	rpm	$10^6 c$ mol/cm^3	$10^{-5} Re_i$	$10^5 St$
.9828	400	4.55	1.000	1.202
.9828	600	4.55	1.499	1.024
.9828	800	4.28	1.999	0.880
.9828	1000	4.28	2.499	0.801
.9828	1200	4.28	2.999	0.733
.9828	1400	4.28	3.499	0.702
.9607	400	4.26	0.955	1.269
.9607	600	4.26	1.433	1.005
.9607	800	4.26	1.910	0.918
.9607	1000	4.26	2.388	0.884
.9607	1200	4.26	2.865	0.836
.9607	1400	4.26	3.343	0.810

exchanged per ion reacting, F Faraday's constant, and c the bulk concentration of the reacting species.

Theory

If shear induced turbulence is postulated, one may expect to describe the friction-factor and mass-transfer behavior with an empirical model, such as the Wasan, Tien, Wilke(15) correlation which was developed to correlate the turbulent mass transfer for flow in pipes and more recently was used to predict closely the mass transfer to rotating disks in turbulent flow.(16,17) This model has been chosen for this study. The eddy diffusivity is correlated as a function of a dimensionless distance from the wall; this distance is

$$y^+ = \frac{y}{\nu}\sqrt{\tau/\rho}\ . \qquad (5)$$

Near the inner cylinder $y_i = r - \kappa R_o$ and the shear stress at the wall $\tau = \tau_i$; r is the radial distance from the center of rotation. Near the outer cylinder, $y_o = R_o - r$ and $\tau = \tau_o$. An angular momentum balance leads to

$$\kappa^2 R_o^2 \tau_i = R_o^2 \tau_o\ . \qquad (6)$$

Since the eddy diffusivity is continuous across the gap, we must determine the value of r at which $y_i^+ = y_o^+$. From equations 5 and 6

$$y^+_{\max} = \kappa R_o \frac{1 - \kappa}{1 + \kappa} \sqrt{\frac{\tau_i}{\rho}} \Big/ \nu \ , \tag{7}$$

where $y^+_{\max}$ is the value of y^+ at the radial position where $y^+_i = y^+_o$. Introducing the friction factor

$$f = \frac{\tau_i}{\frac{1}{2}\, \rho \kappa^2 R_o^2 \Omega^2} \tag{8}$$

and using the gap-distance based Reynolds number, equation 3, we find from equation 7 that

$$y^+_{\max} = \frac{\kappa}{1 + \kappa}\, \mathrm{Re}\, \sqrt{f/2} \ . \tag{9}$$

The shear-stress expression for cylindrical coördinates is,(18) when turbulence is included,

$$\bar{\tau}_{r\theta} = \frac{\tau_i (\kappa R_o)^2}{r^2} = -(\mu + \mu^{(t)})\, r \, \frac{\partial\left(\frac{\bar{v}_\theta}{r}\right)}{\partial r} \ , \tag{10}$$

where μ and $\mu^{(t)}$ are the absolute and eddy viscosities and $\bar{v}_\theta$ is the time-averaged θ-velocity at radial position r . The expression for y^+ and f may be introduced, and equation 10 may be integrated across the gap (considering the outer cylinder stationary) to yield

$$\sqrt{2/f} = \int_0^{y^+_{\max}} \frac{dy^+_i}{\left(1 + \frac{1-\kappa}{1+\kappa}\, \frac{y^+_i}{y^+_{\max}}\right)^3 \left(1 + \frac{\nu^{(t)}}{\nu}\right)} + \int_0^{y^+_{\max}} \frac{\kappa^2\, dy^+_o}{\left(1 - \frac{1-\kappa}{1+\kappa}\, \frac{y^+_o}{y^+_{\max}}\right)^3 \left(1 + \frac{\nu^{(t)}}{\nu}\right)} \tag{11}$$

where the eddy kinematic viscosity is $\nu^{(t)} = \mu^{(t)}/\rho$. The development of the expressions for the mass-transfer rate proceeds in an analogous manner. When the equation for turbulent mass transport in cylindrical coördinates is integrated across the gap, the resultant expression, in terms of the Stanton number, is

$$\sqrt{\frac{f}{2}}\,\frac{1-\kappa^2}{St} = \int_0^{y^+_{max}} \frac{2\,dy^+}{[1-(\alpha y^+)^2]\left(\frac{1}{Sc}+\frac{\mathcal{D}^{(t)}}{\nu}\right)} - \int_0^{y^+_{max}} \frac{[1+\kappa^2-(1-\kappa^2)\alpha y^+]dy^+}{\frac{1}{Sc}+\frac{\mathcal{D}^{(t)}}{\nu}} \; . \qquad (12)$$

$\mathcal{D}^{(t)}$ is the eddy diffusivity; $\mathcal{D}^{(t)}/\nu$ is correlated as a function of y^+ in empirical treatments of turbulent transport.(15,19)

For arbitrary values of Sc and y^+_{max} , these integrals must be evaluated numerically due to the complicated nature of the expressions relating $\mathcal{D}^{(t)}/\nu$ to y^+ . However, in the limit as Sc → ∞ , a singular perturbation expansion of these integrals is possible.(12) When the eddy-diffusivity correlation of Wasan, Tien, Wilke(15) is used, the result is

$$\frac{1}{St}\sqrt{f/2} = \frac{2\pi Sc^{2/3}}{3\sqrt{3}\,A^{1/3}} + Sc^{1/3}\left[\frac{2\pi}{3\sqrt{3}\,y^+_{max}A^{2/3}} + \frac{B}{3A}\,\Gamma\!\left(\frac{5}{3}\right)\Gamma\!\left(\frac{1}{3}\right) - \frac{2\alpha\pi}{3\sqrt{3}}\right] + \frac{1}{3}\left(\frac{\alpha^2}{A} + \frac{B^2}{A^3} - \frac{\alpha B}{A^2} + \frac{B}{y^+_{max}A^2}\right)\log Sc + O(1) \; , \qquad (13)$$

where A and B are constants appearing in the eddy-diffusivity correlation ($A = 9.39\times10^{-4}$ and $B = 1.65\times10^{-5}$) and $\alpha = \frac{1-\kappa}{1+\kappa}\frac{1}{y^+_{max}}$.

This expression converges rapidly for Schmidt numbers on the order of 1000. For $Sc = 1000$ and $y^+_{max} = 100$, the term of order (log Sc) contributes only approximately one percent of the leading term.

Results and Conclusions

The experimental data for $Sc = 1661$ are presented on figure 4 as the Stanton number versus the inner cylinder-radius based Reynolds number Re_i . A comparison of the data gathered for two different Schmidt numbers, $Sc = 1661$ and $Sc = 5780$, is shown on figure 5 as $StSc^{2/3}$ as a function of Reynolds number Re_i for two gap ratios, $\kappa = 0.9829$ and $\kappa = 0.9608$. Except for three points taken with $\kappa = 0.9829$ and $Sc = 1661$, the curves for each gap ratio seem to agree closely. The three errant points differ from the suggested data fit by approximately ten percent (maximum). We may thus conclude that the $Sc^{2/3}$ dependence suggested by the empirical model and verified by Eisenberg(2,3) and others(4-7) provides a good fit of these data. The Reynolds-number dependence of the Stanton number, however, does not seem to agree with these previous studies. It appears from figure 4 that Reynolds number alone does not suffice for an accurate correlation. The systematic trend of reduced transfer rates with reduced gap size would seem to indicate that the influence of the presence of the outer cylinder is beginning to be felt. Figure 6 shows the mass-transfer behavior predicted by equations 11 and 12 when the eddy diffusivity model of Wasan, Tien,

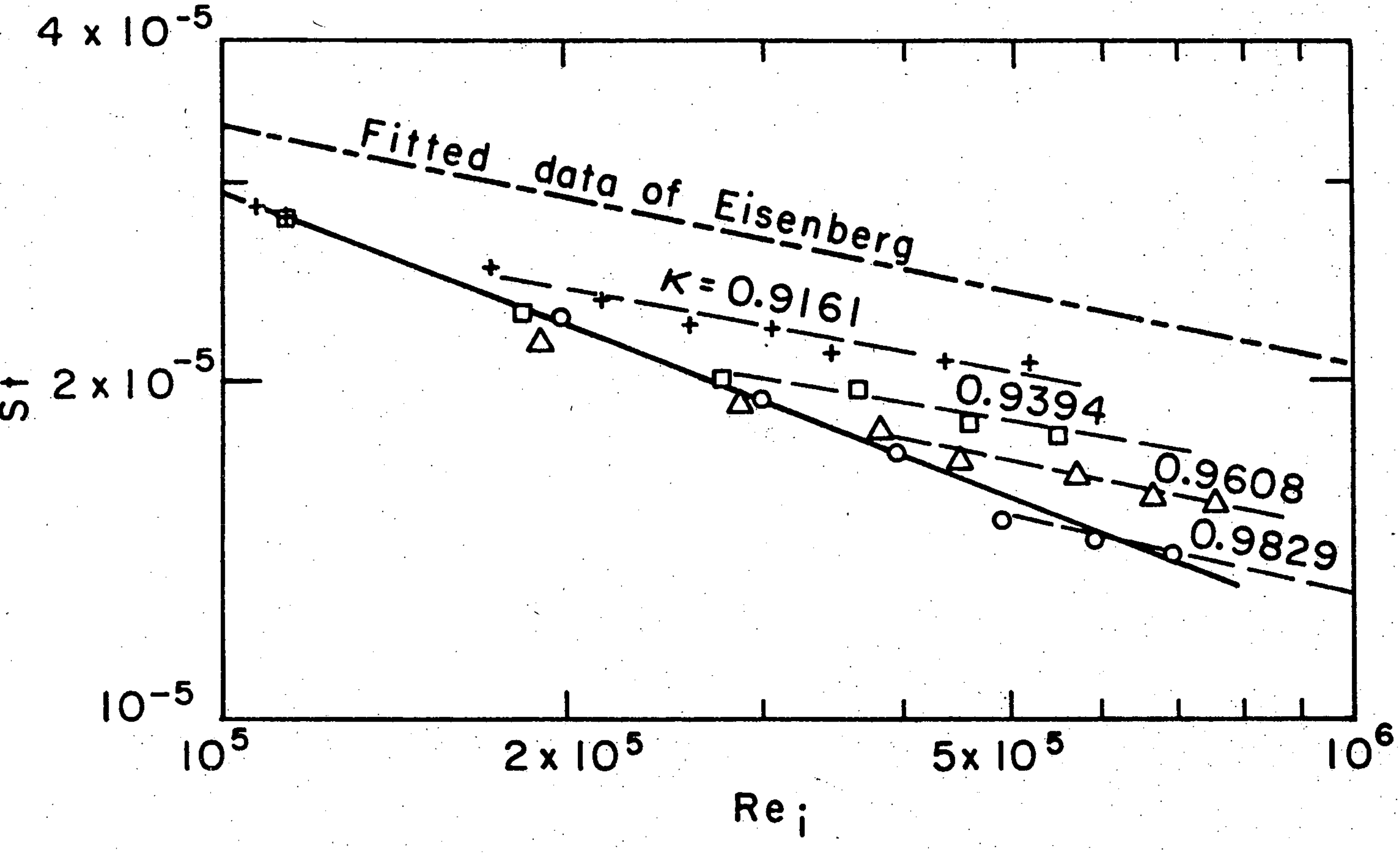

XBL756-3092

Figure 4. Mass-transfer rate for turbulent flow between rotating cylinders.

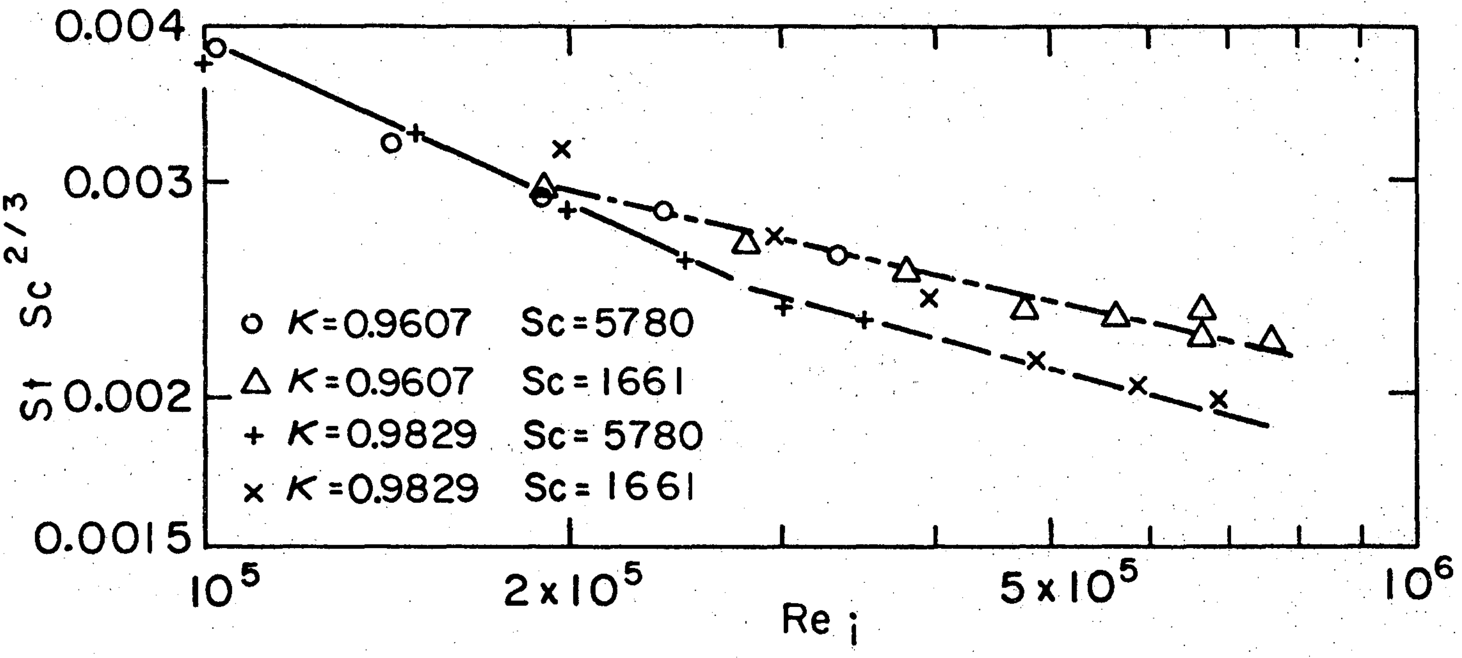

XBL756-3093

Figure 5. Comparison of data for two Schmidt numbers for turbulent flow in a rotating cylinder cell.

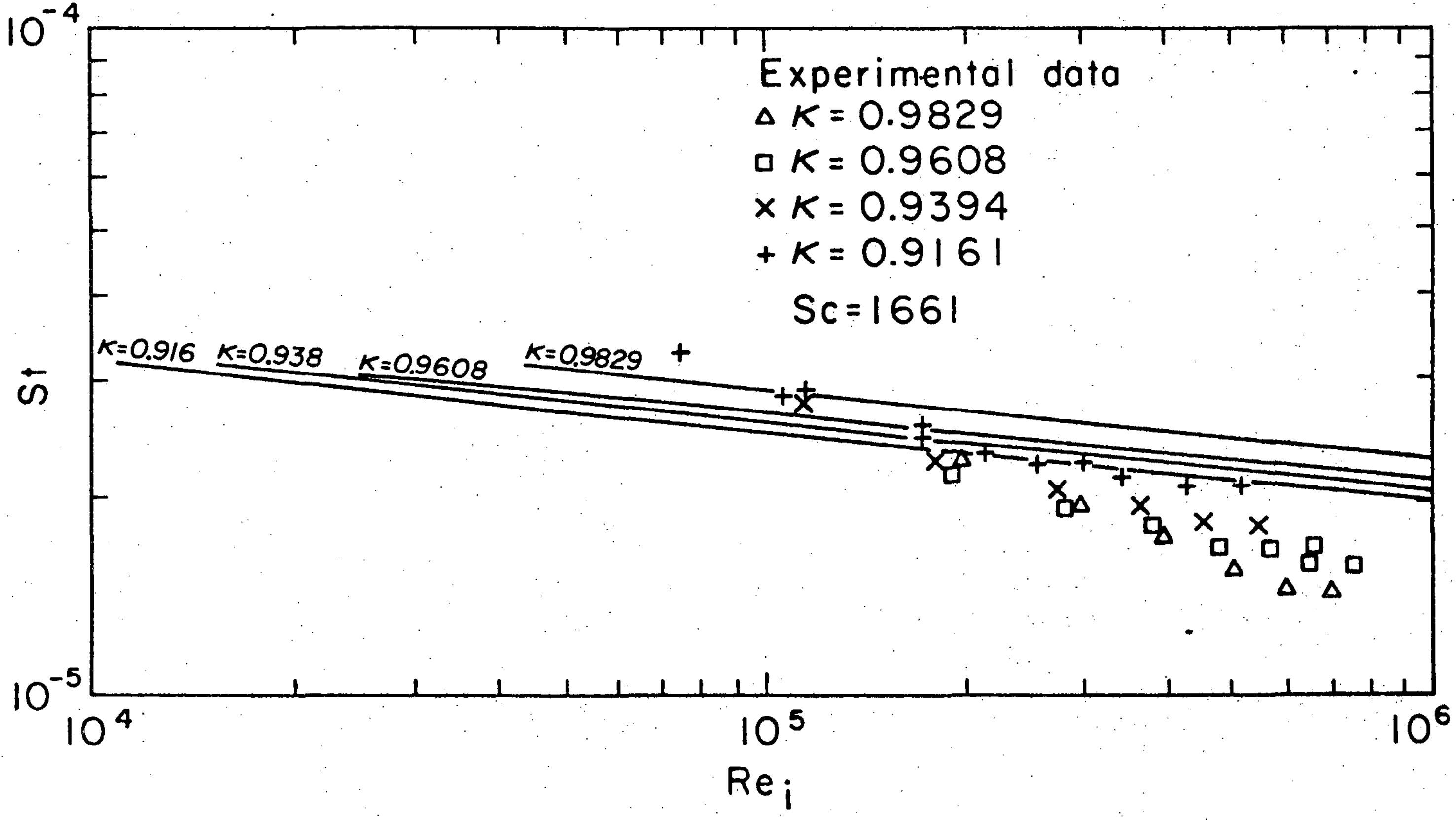

XBL756-3099

Figure 6. Comparison of predicted and experimental mass-transfer rates for small gap conditions with Sc = 1661.

Wilke(15) is used. While the results seem in reasonable agreement for the larger gaps used, it is important to note that they predict a trend that is opposite to that given by the data - an increase in transfer rate as the gap size diminishes rather than the observed decrease. The slope of the predicted curves is considerably less than that found for the data, approximately -0.12 rather than -0.2. The disagreement between predicted and observed transfer rates is more extreme for lower Reynolds numbers. These results suggest that the shear-induced turbulent behavior, upon which the empirical model is based, is not the dominant factor even for the small gaps used in this study. If one adopts the concept that the centrifugal instabilities, such as cause Taylor vortices(9) to form as the laminar Couette flow becomes unstable, are the cause of the turbulence, then it appears that the effect of decreasing the gap between the cylinders serves to dampen the propagation of these turbulent eddies; hence the reduced transfer rate.

As a purely empirical fit of the lines defined by the results for large Reynolds numbers, the data on figure 4 lead to (for Sc = 1661)

$$St = (0.001177 - 0.000983\kappa)Re_i^{-0.2} \tag{14}$$

which is accurate to within approximately five percent. This equation is of interest only in displaying the uniform trend that appears for this limited range of Reynolds numbers and gap ratios. It is also interesting to note that the experimental results of both Eisenberg (for mass transfer) and Theodorsen and Regier (for friction factors) agree with these large Re asymptotes in that they display a Reynolds number dependence of approximately $Re^{-0.2}$ for this range of Reynolds numbers, even though their correlations are given as $Re^{-0.3}$, which provides a better fit for smaller values of Re_i. The modeling based upon a "universal eddy diffusivity" profile has not proven successful for this geometry. While one may speculate that the shear-induced turbulence must dominate for sufficiently small gaps,(11) the construction of electrodes with which to test this hypothesis does not seem feasible. It would appear that further progress in modeling this system must involve a more thorough knowledge of the structure of turbulence in rotating flows.

Acknowledgment

This report was done with support from the United States Energy Research and Development Administration. Any conclusions or opinions expressed in this report represent solely those of the authors and not necessarily those of The Regents of the University of California, the Lawrence Berkeley Laboratory or the United States Energy Research and Development Administration.

Nomenclature

A,B	constants in correlation of eddy diffusivity
c	bulk concentration of ferricyanide ion, mol/cm^3
D	diffusion coefficient of ferricyanide ion, cm^2/s
$\mathcal{D}^{(t)}$	eddy diffusivity, cm^2/s
f	friction factor
F	Faraday's constant, 96487 C/mol
$\bar{i}$	average current density, A/cm^2
n	number of electrons exchanged per ion reacting
r	radial position coördinate, cm
R_i	inner cylinder radius, cm
R_o	outer cylinder radius, cm
Re	Reynolds number based on gap distance
Re_i	Reynolds number based on radius of inner cylinder
$Sc = \nu/D$	the Schmidt number
St	Stanton number
Ta	Taylor number

$\bar{v}_\theta$	time averaged velocity in angular direction, cm/s
y	distance from solid wall, cm
y^+	dimensionless distance from the wall
α	constant defined below equation 13
ε	magnitude of surface irregularities, cm
κ	ratio of inner cylinder radius to outer cylinder radius
μ	viscosity, g/m-s
$\mu^{(t)}$	eddy viscosity, g/m-s
ν	kinematic viscosity, cm^2/s
$\nu^{(t)}$	eddy kinematic viscosity, cm^2/s
ρ	density of the solution, g/cm^3
τ	shear stress, N/m^2
Ω	rotation speed of inner cylinder, rad/s

References

1. D. R. Gabe, "The Rotating Cylinder Electrode," Journal of Applied Electrochemistry, 4, 91-108 (1974).
2. M. Eisenberg, C. Tobias, and C. Wilke, "Mass Transfer at Rotating Cylinders," Chemical Engineering Progress Symposium Series, 16, 1 (1955).
3. M. Eisenberg, Studies on the Role of Ionic Diffusion and Mass Transfer in Electrode Processes, Ph.D. Dissertation, University of California, Berkeley (1954).
4. D. Dropkin and A. Carmi, "Natural-Convection Heat Transfer from a Horizontal Cylinder Rotating in Air," American Society of Mechanical Engineers, Transactions, 79, 741 (1957).
5. R. Kappesser, I. Cornet, and R. Greif, "Mass Transfer to a Rough Rotating Cylinder," Journal of the Electrochemical Society, 118, 1957 (1971).
6. A. J. Arvia and J. S. W. Carozza, "Mass Transfer in the Electrolysis of $CuSO_4 - H_2SO_4$ in Aqueous Solutions under Limiting Current and Forced Convection Employing a Cylindrical Cell with Rotating Electrodes," Electrochimica Acta, 7, 65 (1962).
7. A. J. Arvia, J. S. W. Carozza, and S. L. Marchiano, "The Mechanism of Turbulent Flow in Mass-Transfer Controlled Electrochemical Reactions," Electrochimica Acta, 9, 1483 (1964).
8. T. Theodorsen and A. Regier, "Experiments in Drag of Revolving Disks, Cylinders, and Streamline Rods at High Speeds," United States National Advisory Committee on Aeronautics, Transactions, TR793, 367 (1944).

9. G. I. Taylor, *Philosophical Transactions of the Royal Society of London*, *A223*, 289 (1923).

10. H. Schlicting, *Boundary Layer Theory*, McGraw-Hill Book Co., New York, N.Y. (1968).

11. D. R. Gabe and J. D. Robinson, "Mass Transfer in a Rotating Cylinder Cell - Part II Turbulent Flow," *Electrochimica Acta*, *17*, 1129 (1972).

12. C. Mohr, Jr., *Mass Transfer in Rotating Electrode Systems*, Ph.D. Dissertation, University of California, Berkeley (1975).

13. I. M. Kolthoff, *Industrial and Engineering Chemistry*, *Analytical Edition*, *3*, 381 (1931).

14. E. H. Swift, *A System of Chemical Analysis*, Prentice-Hall, Inc., New York, N.Y. (1939).

15. D. T. Wasan, C. L. Tien, and C. Wilke, "Theoretical Correlation of Velocity and Eddy Viscosity for Flow Close to a Pipe Wall," *American Institute of Chemical Engineers Journal*, *9*, 567 (1963).

16. B. T. Ellison and I. Cornet, "Mass Transfer to a Rotating Disk," *Journal of the Electrochemical Society*, *118*, 68 (1971).

17. B. T. Ellison, *Mass Transfer to a Rotating Disk*, Ph.D. Dissertation, University of California, Berkeley (1969).

18. R. B. Bird, W. E. Stewart and E. N. Lightfoot, *Transport Phenomena*, John Wiley and Sons, Inc., New York, N.Y. (1960).

19. R. G. Deissler, "Analysis of Heat Transfer, Mass Transfer, and Friction in Smooth Tubes at High Schmidt Numbers and Prandtl Numbers," United States National Advisory Committee on Aviation, *Report number 1210*, 69 (1955).

TECHNICAL INFORMATION DIVISION
LAWRENCE BERKELEY LABORATORY
UNIVERSITY OF CALIFORNIA
BERKELEY, CALIFORNIA 94720